

Side Effects of Damping Element Insertion in LCL Filter for DC/AC Inverter

Faizal Arya Samman, Ma'arif Hasan, Tirza Damayanti

Department of Electrical Engineering, Faculty of Engineering
Universitas Hasanuddin, Indonesia

Article Info

Article history:

Received Aug. 18, 2017

Revised Dec. 11, 2017

Accepted Dec. 28, 2017

Keyword:

Power Converter

DC/AC Inverter

Passive Filter

Harmonics

Resonance Damping Circuit

ABSTRACT

The negative impacts or side effects of a damper circuit insertion in an LCL passive filter utilized to filter DC/AC inverters output voltage is presented in this paper. For comparative study, this paper discusses two damping configurations, namely series and parallel damping, as well as the LCL filter without damping element. Four criteria are used to explore the impacts of the damper circuits, i.e. their total harmonic distortions (THDs), the output voltage amplitude, the output power and the power efficiency. Theoretically and empirically shown by previous studies, the damper element insertion in the filter circuit can indeed reduce the peak resonance frequency of the filter in its frequency response curve. Nevertheless, the damper insertion can potentially decrease the inverters power output and power efficiency, voltage output amplitude, and in circumstances cannot improve its THD reduction. The analysis results have shown that the side effects depends also on the load conditions, which are different for each damping circuit configuration.

Copyright © 2018 Institute of Advanced Engineering and Science.

All rights reserved.

Corresponding Author:

Faizal Arya Samman

Universitas Hasanuddin, Faculty of Engineering, Dept. of Electrical Engineering

Kampus Gowa, Jl. Poros Malino Km. 6, Bontomarannu 92171, Sulawesi Selatan, Indonesia

Email: faizalas@unhas.ac.id

1. INTRODUCTION

Nowadays, the increase of electricity demands, the decrease of the fossil fuels supply and the need for cleaner environments have catalyzed the urgent need for renewable energy sources. Renewable energy sources such as solar or sunlight are strategically advantageous for countries having sunny atmospheric conditions, i.e. the countries lies around the earth equatorial area. Meanwhile, researches in the area of solar-cells or photovoltaic (PV) systems have been intensively made with special intention on the improvement of their energy efficiency. In the future, the higher solar efficiency improvement will boost the rapid use the solar cell not only for industries but specially for home scale utilization. The fabrication cost of solar cells should also be decreased to reduce their cost in markets.

Solar-based power plants have been established in many areas and countries. There are some important components of a solar-based power plant. One of them is inverter, beside a charge controller and an energy storage unit such as rechargeable battery. Figure 1a presents a photovoltaic (PV) system with alternating current (AC) load. The charge controller consists of a Maximum Power Point Tracer (MPPT) module and a battery charger circuit. The MPPT module is used to maximize electric energy or power transfer from PV panel to the battery unit. Because most of renewable energies have direct current (DC) power outputs, inverters becomes an important component in a renewable-energy-based power plant. Inverter is an electric device that works to change or convert DC to AC voltages. There are some techniques to design an inverter. One of them is by using a full-bridge circuit incorporating four power electronic switch devices, where four gate terminals of the switching devices are controlled by an electronic control unit.

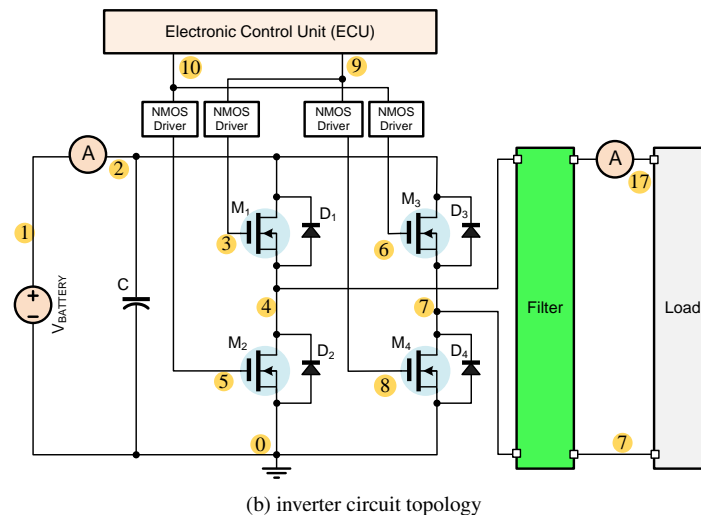
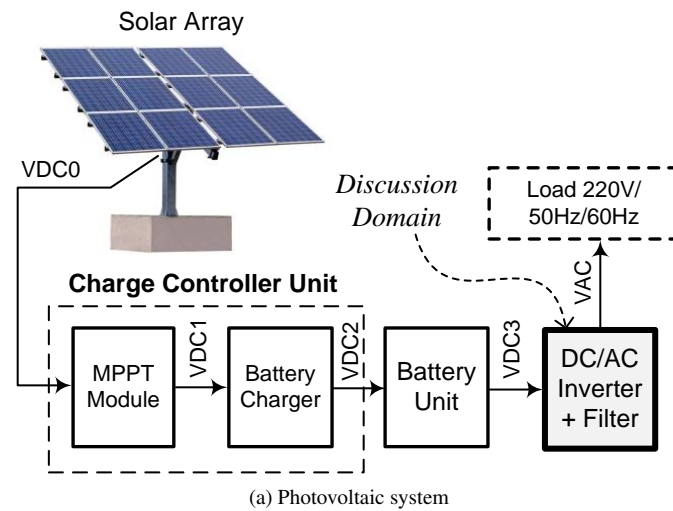


Figure 1. The photovoltaic system and the DC/AC inverter and filter topology.

There many challenging problems in designing an inverter. Some of them are summarized in the following items.

- Power efficiency and switching loss due existing switching mechanism
- Unbalance voltage due to unbalance loads in 3-phase inverter applications
- Voltage amplitude and power factor shifting due to loading conditions
- Grid synchronizations with an existing grid for hybrid power generation
- Total harmonic distortion (THD) due to the used PWM-based switching mechanism to control the inverter output

Most of power losses in switched-mode inverter circuits are due to the existing switching mechanism. Switching pulses applied to the gate terminal of power switching devices will partially convert electrical energy to be thermal energy. Nowadays, new silicon technologies, such as Power MOSFET based on Silicon Carbide (SiC) technology can reduce power losses and have longer operating lifetime [1], [2]. Beside Power MOSFET, another switching device that can be used is *Insulated Gate Bipolar Transistor* or IGBT. Like power MOSFET,

the IGBT operations can also induce higher conduction losses and lower switching performance compared to SiC-based MOSFET [3]. The switching losses as well as electromagnetic interference can be avoided by a new concept i.e. by controlling the current and voltage slopes individually for all operating conditions of the IGBTs [4].

Voltage balancing is also a problem in inverter design especially in grid-connected applications. Stand-alone Micro Grid (MG) tends to have unbalancing voltage affected by the unbalanced load in single phase. To achieve the balancing of phase voltage, each single phase inverter can be controlled independently [5]. Other important aspects in inverter design are the output voltage amplitude, power efficiency and grid synchronization. Grid synchronization is especially very important in 3-phase grid-connected inverter applications [6].

The use of pulse width modulation (PWM) control systems, for instance in AC motor control applications, causes the appearance of common mode voltage (CMV) at the neutral point. CMV suppression and elimination without influencing the inverter's output voltage and better THD can be reached by using a special technique namely Partial elimination SVPWM (PE-SVPWM) and full elimination SVPWM (FE-SVPWM) [7]. The use of a coupled inductor multiplier can also reduce the conduction losses, due to the CMV at neutral point, and raise the efficiency [8]. Z-source T-type inverter is an example way to raise the efficiency system and to boost voltage level without any additional DC-DC converter or transformer. The method makes the output current of inverter are sinusoidal and synchronous with the grid frequency and its phase [9].

Leakage current is the drawbacks of grid-tied transformerless inverter systems. It produces system losses and inject harmonics into the grid [10], [11]. Therefore, the use of passive filter is important to implement. The THD existence causes the inverter output voltage not be able to become pure sine wave as expected. To suppress the harmonic distortion, a passive filter is coupled to the output terminal of the inverter. According to the IEEE Standard, the acceptable THD of the inverter output voltage should be below 5% [12].

There are many filters that can be used to suppress the THD, such as L, LC, LCL, LLCL, etc [13], [14], [15]. Among the aforementioned filters, the LCL filter has better capability to suppress harmonic distortion [16], [15]. Adding an LCL passive filter to the output terminal of an inverter can cause an appearance of peak resonance frequency. This phenomena can make the inverter system unstable and its performance becomes weak. Therefore, to suppress the resonance effect of the LCL passive filter, a resistance component as damper is inserted into the filter circuit. The resistance component inserted to the LCL passive filter is called as a resistance damping [17].

Multi-level inverters are also another type of inverter, which is proposed to reduce harmonics [18], [19] [20]. Multi-level inverter has multiple output voltage levels, which is enabled by the use of multiple DC source. In renewable energy applications, the design cost of a multi-level inverter is higher compared to a single-level inverter, due to the need for more DC/DC converters to maintain the voltage levels of the multiple DC sources. Single-level inverters are still favorable, since they are more simple with lower design cost.

2. RELATED WORKS AND CONTRIBUTION

This paper will particularly discuss an LCL filter analysis. Since the use of LCL passive filter causes the appearance of resonant effect, a damping element is used. By using the damping element, the effect of resonant can be suppressed [17], [21]. However, the resonance damping resistor will raise an extra power loss, reduce maximum voltage amplitude and weaken the high-frequency harmonic reduction capability. This paper will show a comparative study on a few filter circuit with and without damping element. The LCL passive filter with and without the resistance damping tested with resistance loads. The criteria used in this study are the capability of LCL passive filter with and without resistance damping in reducing the harmonic distortion, maintaining the maximum output voltage amplitude and average output power as well as the power efficiency of inverters and filters.

To the best of the author's knowledge, the study of this paper, which is based on concurrent analysis of those four criteria with variable (resistance) loads, has not been explored by the previous works. The work in [17], for example, investigates many filters with active and passive damping methods. The work in [22] proposes different passive damping tuning methods and its analytical damping losses estimation. Nevertheless, both do not expose the impact of the resonance damping element insertion for different load conditions with extra side effects analysis on the THD, power output, power efficiency and the output voltage amplitudes. Variable loading conditions should be taken into account, since in practical conditions, the load is unknown and can potentially affect the load voltage and load current variables. Moreover, the load can be topologically

involved as the part of the filter.

3. RESEARCH METHOD

To achieve the research objective, systematical steps are used to explore the filter and inverter circuit characteristics. The filter and inverter are modeled in (Simulation Program with Integrated Circuit Emphasis). The transfer function of the filter is also mathematically modeled and then numerically modeled to obtain the frequency response curves. By using a SPICE simulator, the inverter+filter circuits are simulated for different load impedance values to measure some parameters and variables, i.e.

1. The THD or total harmonic distortion of the filter output voltages. The analysis is made for 100 harmonic frequency values, where 50 Hz is set as the base frequency.
2. The voltage amplitude values at the inverter's input and output terminals, as well as at the filter output terminal.
3. The average output powers at the inverter's input and output terminals, as well as at the filter output terminal.
4. The power efficiency of the inverter output power over the inverter input power, the filter output power over the inverter output power, and the efficiency of the filter output power over the inverter input power.

After collecting the simulation data, the characteristic curves of all four aforementioned simulation parameters relative to the changes of load impedance values are plotted, and then some concluding remarks are given.

4. FILTER MODELING AND ANALYSIS

The simulated inverter and filter circuit is presented in Figure 1b. The inverter as well as the filter circuit is modeled in SPICE. The electronic control unit (ECU) as shown in the figure generates four sinusoidal pulse width modulation (SPWM) signals. The voltage level of the SPWM signals is amplified using NMOS gate driver such that it can drive the n-channel power MOSFET at the points 3, 5, 6 and 8, respectively as shown in Figure 1b.

Each two of the SPWM signals has similar phase and waveform. The waveform of SPWM signals at the points 3 and 8 is similar, while the other one at the points 5 and 6 is also similar. The NMOS driver increases the voltage level to effectively drive the NMOS gate terminal. In general this driver separates optically the power converter circuit (having higher power) with the electronic control unit (having lower power), or is used to protect the ECU from the higher power circuit.

In order to generate a sine waveform from the output terminal of the inverter, we need to generate some signals to control the process. Normally, this process is made under control of the ECU. The ECU should be programmed to generate two sine-based pulse width modulation (SPWM) as presented by the curves at the second and third line plots in Figure 2. In order to generate the SPWM signals, there are some techniques that can be used. One of them is illustrated from the curves at the first line plot in the Figure 2. An absolute sine wave, called as modulating signal (V_{mod}), is generated having 50 Hz frequency, as well as a carrier signal (V_{carr}) in sawtooth waveform. The figure presents the carrier signal with 20 sawteeth in every half period of the sine wave signal. Both signal are compared each other to generate the SPWM using the following rule. When $V_{carr} > V_{mod}$ then $V_{gate} = 0$, else $V_{gate} = 5 V$. We assume that the logic '1', generated by the ECU, is related to 5 V. During the first half period of the sine wave signal, the SPWM signal is applied to the gates of MOSFET M1 and M4. Then, during the next second half period, the SPWM signal is applied to the gates of MOSFET M2 and M3. Consecutively applying this periodic waveform to the MOSFET gate terminals, then we will have the inverter's output voltage as shown in the fourth line plot in the Figure 2. It seems that the inverter generates AC signal but with large total harmonic distortion (THD).

Because, the output voltage of the inverter contains the THD value larger than 5%, then a filter circuit is required to decrease the THD below 5%. There many types of filters that can be used to suppress the THD. In general, the filter can be classified as active and passive filters. Active filters are rarely used due to the complexity of circuit, especially for high power applications. Passive filters are mostly used in industries because of their

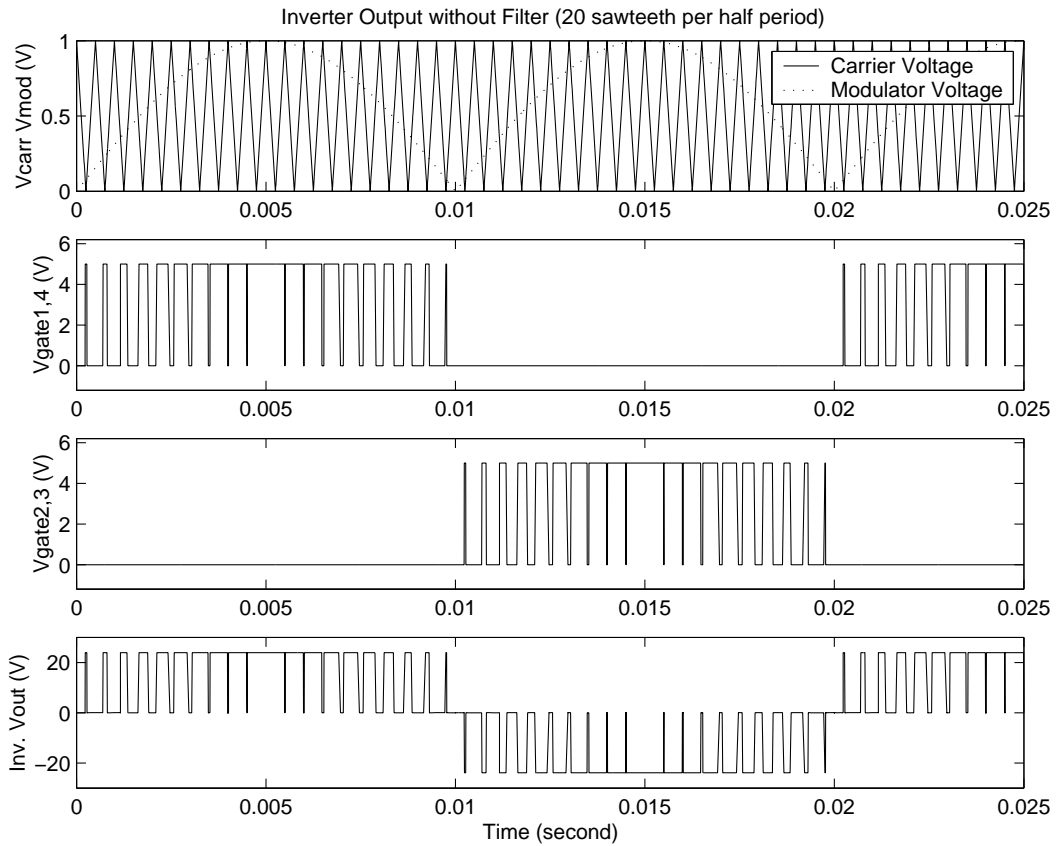


Figure 2. The inverter output signal generation without filter by using 20 sawteeth per half period (The THD of the inverter’s output voltage is 47.829%).

simple use and low cost utilization. the discussion about the used filters to suppress the THD is presented in the following sub section.

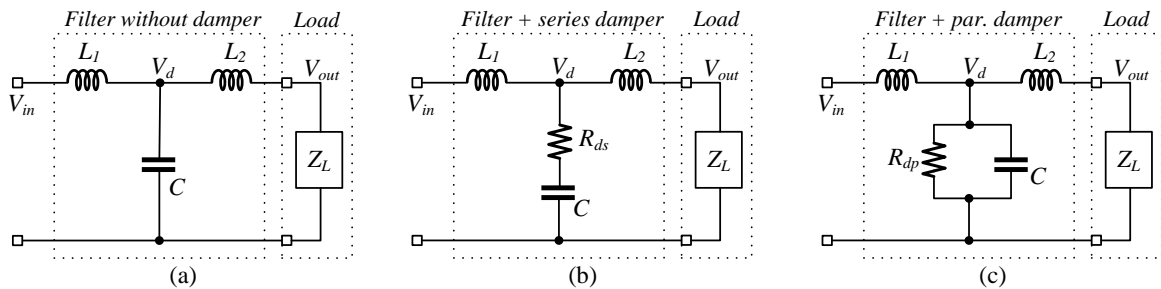


Figure 3. The circuit configuration of the filters under evaluation: (a) filter without damping, (b)(c) filters with passive series and parallel damping methods [17].

4.1. Filter Model without Damper

The filter model without a damper element is presented in Figure 3(a). The transfer function of the $\frac{V_{out}(s)}{V_d(s)}$ is as follows.

$$\frac{V_{out}(s)}{V_d(s)} = \frac{Z_L}{sL_2 + Z_L} \quad (1)$$

The transfer function of the $\frac{V_d(s)}{V_{in}(s)}$ is as follows.

$$\frac{V_d(s)}{V_{in}(s)} = \frac{1}{s^2L_1C + 1} \quad (2)$$

By using the Laplace Transform Characteristic, the transfer function of $\frac{V_{out}(s)}{V_{in}(s)}$ can be obtained by multiplying Eq. (1) and Eq. (2), which results in the following equation.

$$\frac{V_{out}(s)}{V_{in}(s)} = \left(\frac{Z_L}{sL_2 + Z_L} \right) \left(\frac{1}{s^2L_1C + 1} \right) \quad (3)$$

Simplifying Eq. (3), we will have the final transfer function form, i.e.

$$\frac{V_{out}(s)}{V_{in}(s)} = \frac{Z_L}{s^3L_1L_2C + s^2Z_L L_1C + sL_2 + Z_L} \quad (4)$$

4.2. Filter Model with Series Damper

The filter model with a damper element inserted in series with the C-element of the filter is presented in Figure 3(b). Z_{ds} is obtained by deriving the equivalent impedance between the C-element and the series resistant damper R_{ds} , i.e.

$$Z_{ds} = R_{ds} + \frac{1}{sC} = \frac{sR_{ds}C + 1}{sC} \quad (5)$$

The transfer function of the $\frac{V_{out}(s)}{V_d(s)}$ is the same result presented in Eq. (1). The transfer function of the $\frac{V_d(s)}{V_{in}(s)}$ is as follows.

$$\frac{V_d(s)}{V_{in}(s)} = \frac{Z_{ds}}{sL_1 + Z_{ds}} = \frac{sR_{ds}C + 1}{s^2L_1C + sR_{ds}C + 1} \quad (6)$$

By using the Laplace Transform Characteristic, the transfer function of $\frac{V_{out}(s)}{V_{in}(s)}$ can be obtained by multiplying Eq. (1) and Eq. (6), which results in the following equation.

$$\frac{V_{out}(s)}{V_{in}(s)} = \left(\frac{Z_L}{sL_2 + Z_L} \right) \left(\frac{sR_{ds}C + 1}{s^2L_1C + sR_{ds}C + 1} \right) \quad (7)$$

Simplifying Eq. (7), we will have the final transfer function form, i.e.

$$\frac{V_{out}(s)}{V_{in}(s)} = \frac{sZ_LR_{ds}C + Z_L}{s^3L_1L_2C + s^2(Z_LR_1C + R_{ds}L_2C) + s(L_2 + Z_LR_{ds}C) + Z_L} \quad (8)$$

4.3. Filter Model with Parallel Damper

The filter model with a damper element inserted in parallel with the C-element of the filter is presented in Figure 3(c). Z_{dp} is obtained by deriving the equivalent impedance between the C-element and the series resistant damper R_{dp} , i.e.

$$Z_{ds} = \frac{R_{dp} \frac{1}{sC}}{R_{dp} + \frac{1}{sC}} = \frac{R_{dp}}{sR_{dp}C + 1} \quad (9)$$

The transfer function of the $\frac{V_{out}(s)}{V_d(s)}$ is the same result presented in Eq. (1). The transfer function of the $\frac{V_d(s)}{V_{in}(s)}$ is as follows.

$$\frac{V_d(s)}{V_{in}(s)} = \frac{Z_{dp}}{sL_1 + Z_{dp}} = \frac{R_{dp}}{s^2 R_{dp} L_1 C + sL_1 + R_{dp}} \quad (10)$$

By using the Laplace Transform Characteristic, the transfer function of $\frac{V_{out}(s)}{V_{in}(s)}$ can be obtained by multiplying Eq. (1) and Eq. (10), which results in the following equation.

$$\frac{V_{out}(s)}{V_{in}(s)} = \left(\frac{Z_L}{sL_2 + Z_L} \right) \left(\frac{R_{dp}}{s^2 R_{dp} L_1 C + sL_1 + R_{dp}} \right) \quad (11)$$

Simplifying Eq. (11), we will have the final transfer function form, i.e.

$$\frac{V_{out}(s)}{V_{in}(s)} = \frac{Z_L R_{dp}}{s^3 R_{dp} L_1 L_2 C + s^2 (L_1 L_2 + Z_L R_{dp} L_1 C) + s (Z_L L_1 + R_{dp} L_2) + Z_L R_{dp}} \quad (12)$$

4.4. Frequency Response Characteristic

After obtaining the transfer function of the filter circuits with three different damping element configuration, including the one without damping element, then this subsection presents the frequency response characteristic of the filters. Figure 4 presents the bode plot comparison of the filter circuits.

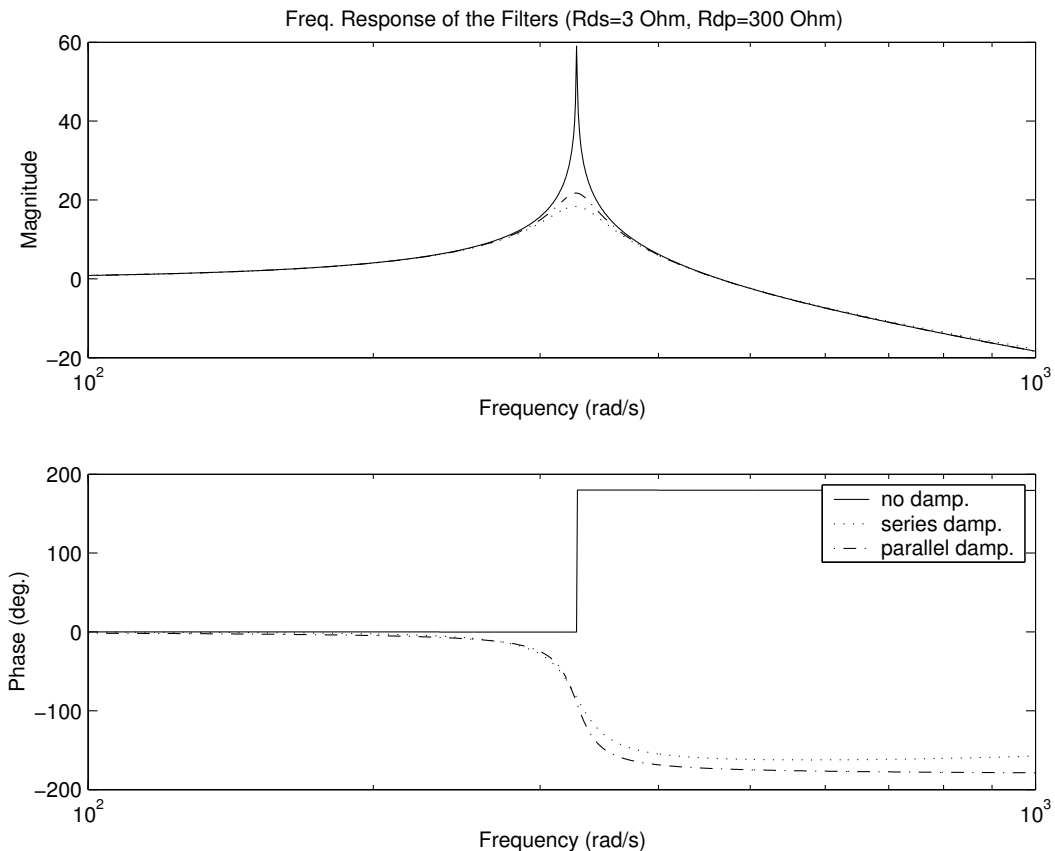


Figure 4. The transfer function of the filter with and without damping.

5. SIMULATION RESULTS AND ANALYSIS

The steady-state and transient analysis or simulation results of some important measured variables in the inverter plus filter configurations are presented in this section. the simulations are made using SPICE

(Simulation Program with Integrated Circuit Emphasis), which is an industry standard circuit simulator. The measured parameters are inverter's and filter's output voltages, output currents, output powers including the average output powers. The THD and power efficiency measurements of the inverter and filter circuit are also made in the analysis.

5.1. Steady-State Point Analysis

In this steady state point analysis or simulation, the measured parameters are THD, voltage and current amplitudes, output power and power efficiencies. In every simulation run, the circuit is simulated until the steady-state condition is attained, and then, the parameters are observed from the SPICE output probe windows. The simulation results are shown in the following sub sections.

5.1.1. THD and Voltage Amplitude Measurements

The upper section of Figure 5 shows the THD measurements at the filter's output points. Each figure presents three THD curves comparisons between the inverter+filter circuits without damping, with series damping and with parallel damping for different resistance loads, i.e. from $10^0\Omega$ until $10^5\Omega$. As shown in the figure, the filter without damping element presents the best THD values, when the load impedance is above 20Ω . Below that impedance value, the filters with damping elements have better THD values, but all of them have THD above 5%, the standardized THD limit.

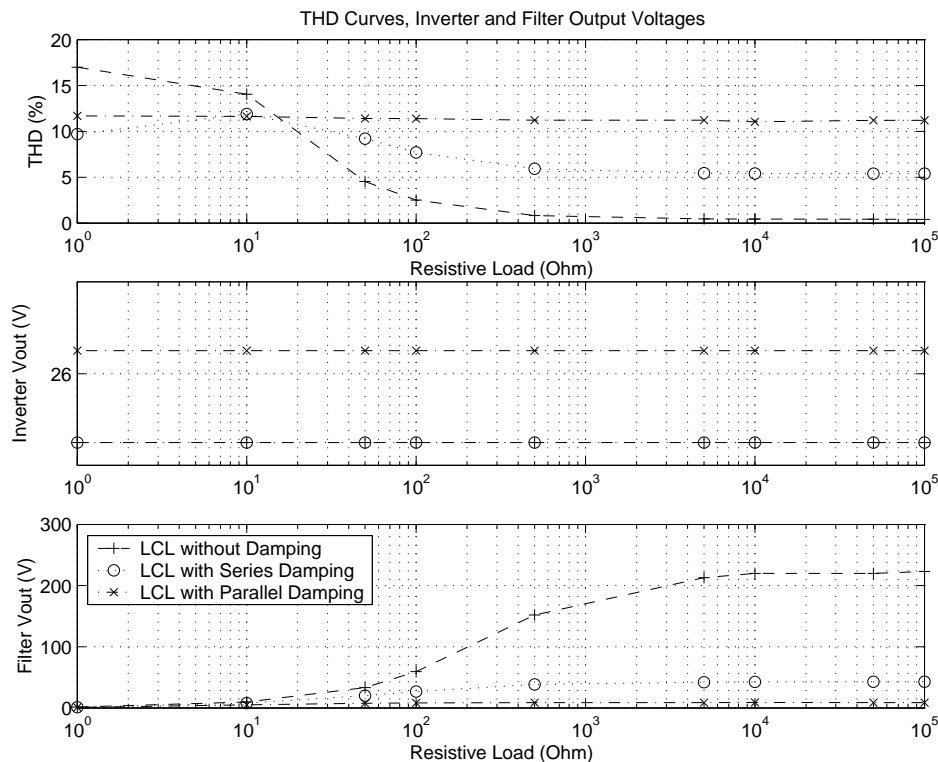


Figure 5. The THD measurements.

The middle and lower sections of Figure 5 shows the voltage amplitude measurements at the inverter's and filter's output points. Each figure presents the curves comparisons between the inverter+filter circuits without damping, with series damping and with parallel damping for different resistance loads, i.e. from $10^0\Omega$ until $10^5\Omega$. The voltage measurements at the inverter's input terminal are not presented, since they present equal value, i.e. 24 V for each aforementioned resistance load value.

The filter output voltage amplitudes of the circuit without damping element presents higher values compared to the filters with series and parallel damping element, especially for the load impedance above $10\ \Omega$. For the load impedance below $10\ \Omega$, all filter circuit presents almost the same results.

5.1.2. Current Measurements

Figure 6 shows the current measurements at the inverter's and filter's input-output points. Each figure presents three current curves comparisons between the inverter+filter circuits without damping, with series damping and with parallel damping for different resistance loads, i.e. from $10^0\ \Omega$ until $10^5\ \Omega$. At the upper part of the figure, the current measurements at the inverter's input terminal are presented. At the middle part of the figure, the current measurements at the inverter's output terminal are presented. At the bottom part of the figure, the current measurements at the filter's output terminal are presented.

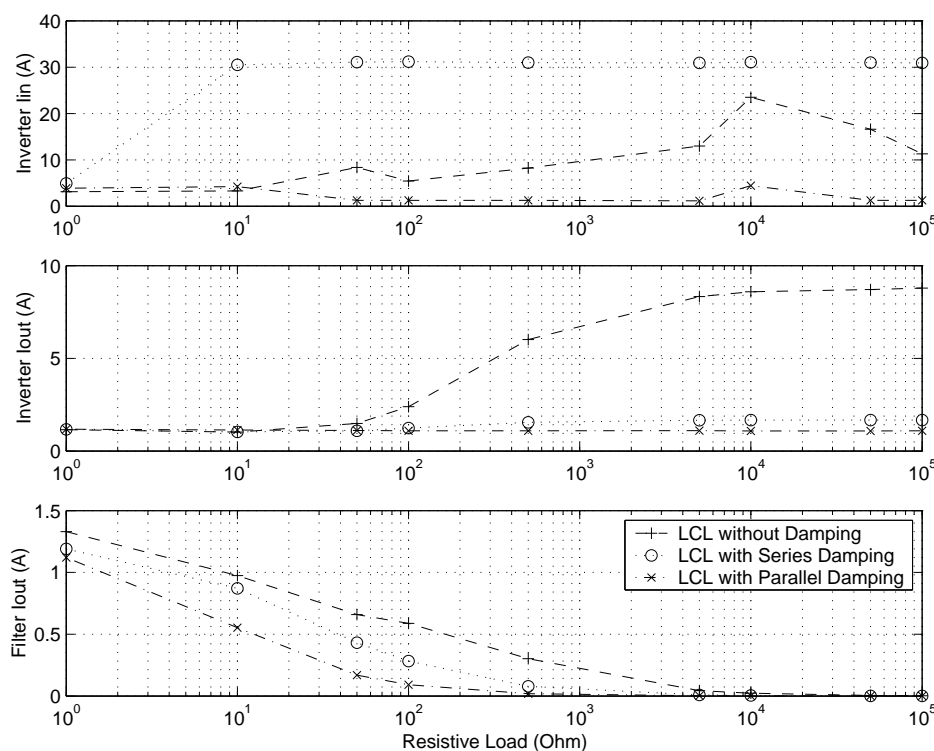


Figure 6. The current measurements.

As shown in Figure 6, the circuit with series damping element has better inverter input currents compared to the circuit without damping element and the circuit with parallel damping element. For the load impedance above $50\ \Omega$, the circuit without damping element has the best inverter output currents. The almost similar values are presented for the load impedance below $50\ \Omega$. For the load impedance below $5\text{k}\Omega$, the output current of the filter without damping element has the highest current values. The almost similar filter output current are presented for the load impedance above $5\text{k}\Omega$.

5.1.3. Power Measurements

Figure 7a shows the power measurements at the inverter's and filter's input-output points. Each figure presents three power curves comparisons between the inverter+filter circuits without damping, with series damping and with parallel damping for different resistance loads, i.e. from $10^0\ \Omega$ until $10^5\ \Omega$. At the upper part of the figure, the power measurements at the inverter's input terminal are presented. At the middle part of the figure, the curves present the power measurements at the inverter's output terminal. At the bottom part of the figure, the power measurements at the filter's output terminal are presented.

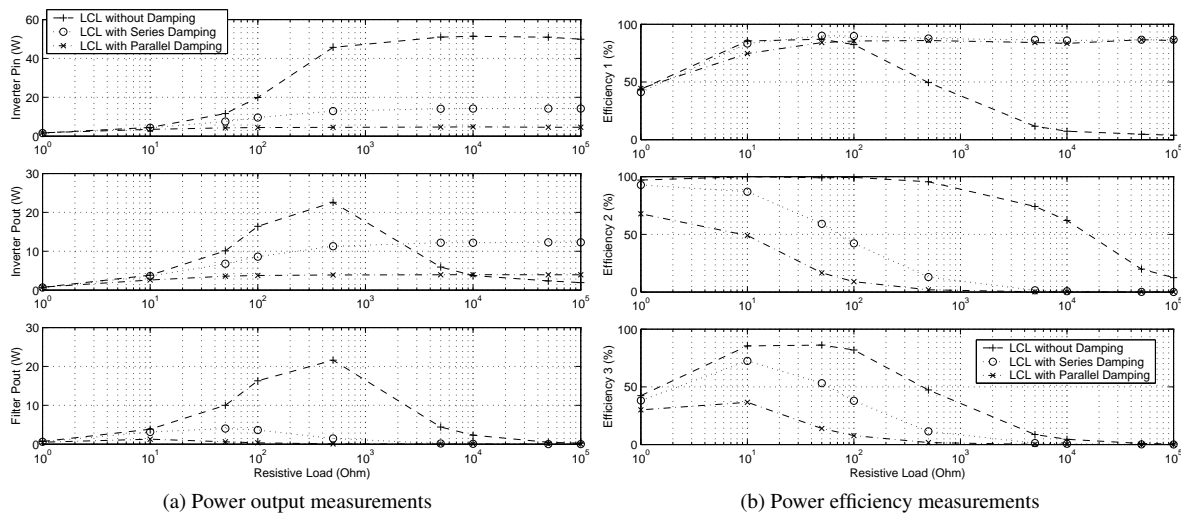


Figure 7. The power output and power efficient measurements.

The inverter input power values of the circuit without damping element are higher than the inverter input power of the circuit with damping elements for all load impedance value. For the load impedance below $2\text{k}\Omega$, the inverter output power values of the circuit without damping element are higher than the other configurations. However, for the load impedance values above $2\text{k}\Omega$, the series damping element circuit configuration presents the highest inverter output power values. The filter without damping element has the higher output power compared to the other circuits with damping elements.

5.1.4. Power Efficiency Measurements

The efficiency curves for the inverter and the filter are presented in Figure 7b. Each figure presents three efficiency curves comparisons between the inverter+filter circuits without damping, with series damping and with parallel damping for different resistance loads, i.e. from $10^0\Omega$ until $10^5\Omega$.

Efficiency 1 is the power efficiency of the inverter output power over the inverter input power, as presented in the upper part of the Figure 7b. In this case, the filters with damping elements have the highest power efficiency compared to the power efficiency of the filter without damping element for the load impedance values about 80Ω . For the load impedance values below 80Ω , power efficiency values of the circuit without damping element are almost the same as the values of the circuit with series damping element, but higher than the values of the circuit with parallel damping element.

Efficiency 2 is the power efficiency of the filter output power over the inverter output power, as presented in the middle part of the Figure 7b. In this case, the power efficiency of the circuit without damping element is higher than the circuits with series and parallel damping elements for all load impedance values.

Efficiency 3 is the power efficiency of the filter output power over the inverter input power, as presented in the bottom part of the Figure 7b. In this case, the power efficiency of the circuit without damping element is higher than the circuits with series and damping elements. The highest power efficiency is shown to be around 10 until 100Ω .

5.2. Transient Analysis

In this subsection, the transient responses of the inverter's output voltage, current, power and average power are presented. The transient responses for the three filter configuration, i.e. without damping, with parallel and series damping are presented and compared directly.

Figure 8 shows the transient response curves, from upper until lower part of the figure, respectively for the output voltage the output current, output power and the average output power of the filter circuit without damper and with damper element. The load impedance is set to 500Ω for both simulations. As presented in

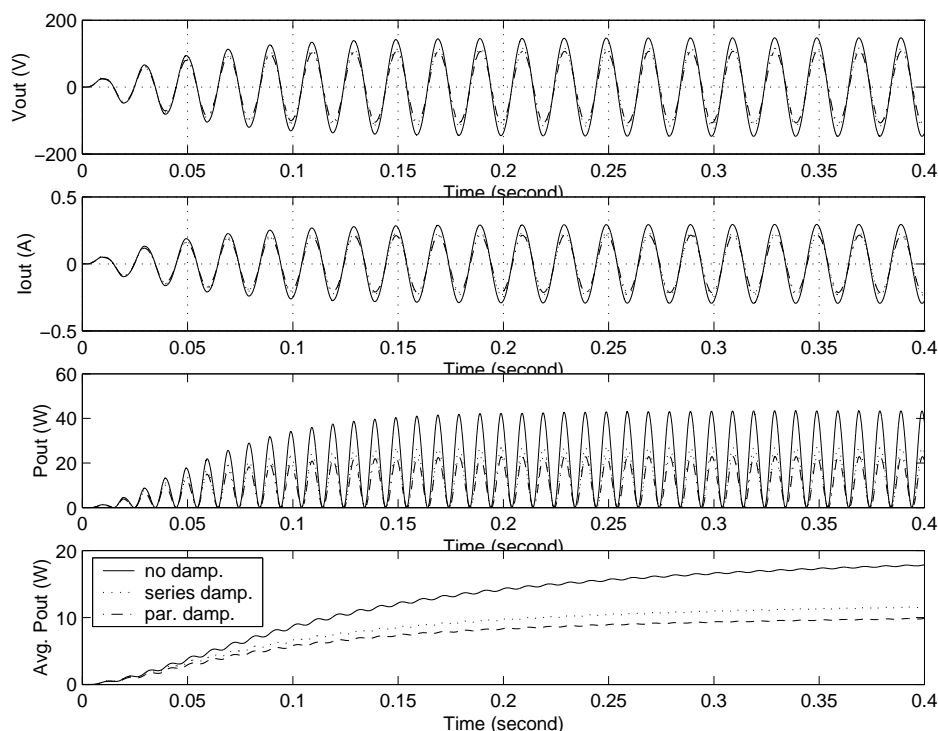


Figure 8. Transient analysis of the filter's output voltage and average power with and without damping with load impedance $Z_{load} = 500\Omega$.

Figure 8, it seems that the filter without damping element has better voltage amplitude compared to the filters with the damper elements. The same result is presented for the average output powers. Compared to the parallel damped filter, the series damped filter shows better average power.

6. CONCLUSION AND OUTLOOKS

This paper has presented the side effects of the damping element insertion in the passive LCL filters. Passive damping method with series configuration can indeed reduce peak resonance frequency. But, in case of higher damping resistor values, the insertion of a resistor in series with the capacitor in the LCL filter circuit as a damper element has disadvantages of decreasing the filter ability in eliminating its THD. It also decreases in the output voltage and reduces the average output power. The output voltage and the average power however can be still improved by choosing appropriate damping resistance values.

In case of parallel damper element insertion in the filter with lower damping resistor values, the same drawbacks appear as same as the previous series damping configuration. It decreases the ability of the filter in reducing harmonics and drops the output voltage amplitude. The dropped output voltage depends on the resistance load value. The dropped voltage becomes larger as the resistance load is larger, but it tends to be steady for relatively larger resistance loads. Output voltage and average power, however, can be still improved by choosing appropriate damping resistance values. Larger resistance damper insertion can surely increase the power losses.

In general, both damping methods (series and parallel damping) can indeed reduce resonance, in which the resonance effect can potentially reduce the filter system stability. However, based on this study, the methods should be applied carefully because it potentially gives negative impacts or side effects in terms of THD, the maximum output voltage (voltage amplitude), the inverters average output power and the power efficiency of the inverter and filter circuits. The impacts are also dependent on the resistance load values.

Load conditions should be considered in the filter modeling, since the load can be topologically involved as the part of the filter. Unfortunately, in practical conditions, the load is unknown. But, theoretically,

the load can be classified as pure resistance loads, loads causing leading current and loads causing lagging current. Hence, a filter that can be tuned over different load condition is required to maintain the inverter performance over the aforementioned criteria.

ACKNOWLEDGEMENT

The authors gratefully acknowledge the Ministry for Research, Technology and Higher Education of the Republic of Indonesia for funding our research work under the scheme of “Post-Graduated Collegium Research Grant” (*Hibah Penelitian Tim Pasca Sarjana*) with Grant Contract No. 005/SP2H/LT/DPRM/IV/2017 in the year 2017.

REFERENCES

- [1] J. Biela, M. Schweizer, S. Waffler, and J. W. Kolar, “SiC versus Si Evaluation of Potentials for Performance Improvement of Inverter and DCDC Converter Systems by SiC Power Semiconductors,” *IEEE Trans. on Industrial Electronics*, vol. 58, no. 7, pp. 2872–2882, July 2011.
- [2] T. Ueda, “GaN, SiC Tout as Next Generation Power Switching Devices,” *AEI Magazine, Tech-Focus*, pp. 38–41, Nov. 2015.
- [3] G. Sena, R. Marani, G. Gelao, and A. G. Perri, “A Comparative Study of Power Semiconductor Devices for Industrial PWM Inverters,” *International Journal of Power Electronics and Drive System (IJPEDES)*, vol. 7, no. 4, pp. 1420–1428, Dec. 2016.
- [4] Y. Lobsiger and J. W. Kolar, “Closed-Loop di/dt and dv/dt IGBT Gate Driver,” *IEEE Trans. on Power Electronics*, vol. 30, no. 6, pp. 3402–3417, June 2015.
- [5] R. M. Kamel, “New inverter control for balancing standalone micro-grid phase voltages: A review on MG power quality improvement,” *Elsevier, Renewable and Sustainable Energy Reviews*, vol. 63, pp. 520–532, Sept. 2016.
- [6] M. G. Villalva, T. de Siqueira, M. Espindola, and E. Ruppert, “Modeling And Control Of A Three-Phase Isolated Grid-Connected Converter For Photovoltaic Applications,” *Revista Controle and Automacao*, vol. 22, no. 3, pp. 215–228, May–June 2011.
- [7] C. Bharatiraja, S. Jeevananthan, J. Munda, and R. Latha, “Improved SVPWM vector selection approaches in OVM region to reduce common-mode voltage for three-level neutral point clamped inverter,” *Elsevier, Electrical Power and Energy Systems*, vol. 79, pp. 285–297, July 2016.
- [8] Y. Zhao, X. Xiang, C. Li, Y. Gu, W. Li, and X. He, “Single-Phase High Step-up Converter With Improved Multiplier Cell Suitable for Half-Bridge-Based PV Inverter System,” *IEEE Trans. on Power Electronics*, vol. 29, no. 6, pp. 2807–2816, June 2014.
- [9] S. Ozdemir, “Z-source T-type inverter for renewable energy systems with proportional resonant controller,” *Elsevier, International Journal of Hydrogen Energy*, vol. 10.1016/j.ijhydene.2016.01.140, no. article in press, pp. 1–12, 2016.
- [10] M. Azril and N. A. Rahim, “Design Analysis of Low-Pass Passive Filter In Single-Phase Grid-Connected Transformerless Inverter,” in *Proc. of the IEEE First Conference On Clean Energy And Technology (CET)*, 2011, pp. 348–353.
- [11] B. Gu, J. Dominic, J.-S. Lai, C.-L. Chen, T. LaBella, and B. Chen, “High Reliability and Efficiency Single-Phase Transformerless Inverter for Grid-Connected Photovoltaic Systems,” *IEEE Trans. on Power Electronics*, vol. 28, no. 5, pp. 2235–2245, May 2013.
- [12] M. Hojabri and A. Toudeshki, “Third-Order Passive Filter Improvement for Renewable Energy Systems to Meet IEEE 519-1992 Standard Limits,” pp. 199–204, 2015.
- [13] M. Elsharty and H. Ashour, “Passive L And LC Filter Design Method For Grid Connected Inverter,” in *Proc. of the IEEE Innovative Smart Grid Technologies Asia (ISGT-ASIA)*, 2014, pp. 13–18.
- [14] W. Wu, Y. Sun, M. Huang, X. Wang, H. Wang, F. Blaabjerg, M. Liserre, and H. S.-H. Chung, “A Robust Passive Damping Method For LLCL-Filter-Based Grid-Tied Inverters To Minimize The Effect Of Grid Harmonic Voltages,” *IEEE Trans. on Power Electronics*, vol. 29, no. 7, pp. 3279–3289, July 2014.
- [15] F. A. Samman and A. Azhari, “DC/AC Power Converter for Home Scale Electricity Systems Powered by Renewable Energy,” in *Proc. of the 3rd IEEE Int’l Conf. on Smart Green Technology in Electrical and Information Systems (ICSGTEIS)*, 2016, pp. 149–154.

- [16] W. Wu, Y. He, T. Tang, and F. Blaabjerg, "A New Design Method for the Passive Damped LCL- and LLCL-Filter Based Single-Phase Grid-tied Inverter," *IEEE Trans. on Industrial Electronics*, vol. 60, no. 10, pp. 4339–4350, Oct. 2013.
- [17] M. Buyuk, A. Tan, M. Tumay, and K. Bayndr, "Topologies, Generalized Designs, Passive And Active Damping Methods of Switching Ripple Filters For Voltage Source Inverter: A Comprehensive Review," *Elsevier, Renewable and Sustainable Energy Reviews*, vol. 62, pp. 46–69, Sept. 2016.
- [18] H. M. Bassi, "A Modulation Scheme for Floating Source Multilevel Inverter Topology with Increased Number of Output Levels," *International Journal of Electrical and Computer Engineering (IJECE)*, vol. 6, no. 5, pp. 1985–1993, Oct. 2016.
- [19] R. Benioub, L. Kadri, M. Adnane, and K. Itaka, "Modulation Index Variation Effect on Harmonic Behavior of Fifteen Multilevel Inverter Neutral-Point-Clamped Topology," *International Journal of Electrical and Computer Engineering (IJECE)*, vol. 7, no. 4, pp. 1892–1898, Aug. 2017.
- [20] N. H. Ramlan, N. A. Azli, and N. F. A. A. Hafidz, "Performance of Interconnection and Damping Assignment Passivity-Based Controller on Inverter Circuits," *International Journal of Power Electronics and Drive System (IJPEDS)*, vol. 8, no. 1, pp. 69–80, Mar. 2017.
- [21] J. Muhlethaler, M. Schweizer, R. Blattmann, J. W. Kolar, and A. Ecklebe, "Optimal design of LCL harmonic filters for three-phase PFC rectifiers," *IEEE Trans. on Power Electronics*, vol. 28, no. 7, pp. 3114–3125, July 2013.
- [22] R. Pena-Alzola, M. Liserre, F. Blaabjerg, R. Sebastian, J. Dannehl, and F. W. Fuchs, "Analysis of the Passive Damping Losses in LCL-Filter-Based Grid Converters," *IEEE Trans. on Power Electronics*, vol. 28, no. 6, pp. 2642–2646, June 2013.

BIOGRAPHIES OF AUTHORS



Faizal Arya Samman received his Bachelor of Engineering degree in Electrical Engineering (with honors) from Universitas Gadjah Mada (UGM), Yogyakarta in 1999 and his Master of Engineering degree from Institut Teknologi Bandung (ITB) in 2002. In 2002 he was appointed to be a research and teaching staff at Faculty of Engineering, Universitas Hasanuddin in Makassar, Indonesia. He received a scholarship award (2006–2010) from Deutscher Akademischer Austausch-Dienst (DAAD, German Academic Exchange Service) to pursue his Doktor-Ingenieur degree at Technische Universität Darmstadt (TUD), Germany. From 2010 until 2012 he worked as the postdoctoral research fellow in LOEWE-Zentrum AdRIA (Adaptronik-Research, Innovation, Application) at Fraunhofer Institut LBF Darmstadt. His research interests include FPGA-based digital systems design, power electronics, network on-chip (NoC), systems-on-chip (SoC), and multi-core embedded computer systems.



Ma'arif Hasan finished his Bachelor degree (with honors) in 2017 from Universitas Hasanuddin at Department of Electrical Engineering, with major study in the field of power system engineering. His research interests are power electronic converter and renewable energy systems.



Tirza Damayanti finished her Bachelor degree (with honors) in 2017 from Universitas Hasanuddin at Department of Electrical Engineering, with major study in the field of telecommunication engineering. Her research interests are electric and electronic circuit analysis and filter circuit design.